SECURITY CLASSIFICATION OF THIS PAGE

## REPORT DOCUMENTATION PAGE

Form Approved
OMB No. 0704-0188

| | |
|---|---|
| 1a REPORT SECURITY CLASSIFICATION<br>UNCLASSIFIED | 1b RESTRICTIVE MARKINGS |
| 2a SECURITY CLASSIFICATION AUTHORITY | 3 DISTRIBUTION / AVAILABILITY OF REPORT<br>Approved for public release; distribution unlimited. |
| 2b DECLASSIFICATION / DOWNGRADING SCHEDULE | |
| 4 PERFORMING ORGANIZATION REPORT NUMBER(S)<br>NRL Report 9100 | 5 MONITORING ORGANIZATION REPORT NUMBER(S) |
| 6a NAME OF PERFORMING ORGANIZATION<br>Naval Research Laboratory<br>6b OFFICE SYMBOL (If applicable) | 7a NAME OF MONITORING ORGANIZATION |
| 6c ADDRESS (City, State, and ZIP Code)<br>Washington, DC 20375-5000 | 7b ADDRESS (City, State, and ZIP Code) |
| 8a NAME OF FUNDING / SPONSORING ORGANIZATION<br>Office of Naval Research<br>8b OFFICE SYMBOL (If applicable) | 9 PROCUREMENT INSTRUMENT IDENTIFICATION NUMBER |
| 8c ADDRESS (City, State, and ZIP Code)<br>Arlington, VA 22217 | 10 SOURCE OF FUNDING NUMBERS<br>PROGRAM ELEMENT NO: 61153N; PROJECT NO: 021-05-43; TASK NO: ; WORK UNIT ACCESSION NO: DN480-006 |

11 TITLE (Include Security Classification)
Nearfield Detection of a Crossing Target in Clutter

12 PERSONAL AUTHOR(S)
Broder, Bruce

| 13a TYPE OF REPORT | 13b TIME COVERED | 14 DATE OF REPORT (Year, Month, Day) | 15 PAGE COUNT |
|---|---|---|---|
| Interim | FROM _____ TO _____ | 1987 November 27 | 12 |

16 SUPPLEMENTARY NOTATION
(See Page ii)

| 17 COSATI CODES | | | 18 SUBJECT TERMS (Continue on reverse if necessary and identify by block number) |
|---|---|---|---|
| FIELD | GROUP | SUB-GROUP | Radar signal processing<br>MTI<br>Array processing |
| | | | |
| | | | |

19 ABSTRACT (Continue on reverse if necessary and identify by block number)

The detection of a crossing target in the nearfield in Gaussian clutter is explored. The relative phase shifts across antenna elements are nonlinear functions of the geometry and change through time. Consequently, crossing targets in the nearfield exhibit a changing phase called spatial Doppler and can be separated from the highly correlated clutter. By using two examples, the signal-to-noise ratio is shown to be significantly enhanced for the crossing target in clutter.

| 20 DISTRIBUTION / AVAILABILITY OF ABSTRACT | 21 ABSTRACT SECURITY CLASSIFICATION | |
|---|---|---|
| ☒ UNCLASSIFIED/UNLIMITED ☐ SAME AS RPT. ☐ DTIC USERS | UNCLASSIFIED | |
| 22a NAME OF RESPONSIBLE INDIVIDUAL<br>Ben H. Cantrell | 22b TELEPHONE (Include Area Code)<br>(202) 767-2573 | 22c OFFICE SYMBOL<br>Code 5312 |

DD Form 1473, JUN 86 *Previous editions are obsolete.* SECURITY CLASSIFICATION OF THIS PAGE

S/N 0102-LF-014-6603

16. SUPPLEMENTARY NOTATION

B. Broder is a graduate student in the Department of Electrical Engineering, Princeton University, Princeton, NJ 08544 and is supported by an Office of Naval Research (ONR) fellowship. This work was performed at the Radar Analysis Branch, Radar Division, Naval Research Laboratory, Washington, DC 20375-5000 under the ONR fellowship program.

Naval Research Laboratory
Washington, DC 20375-5000

NRL Report 9100



# Nearfield Detection of a Crossing Target in Clutter

BRUCE BRODER

*Radar Analysis Branch*
*Radar Division*

November 17, 1987

## CONTENTS


INTRODUCTION ..... 1

EXAMPLE 1 ..... 1

EXAMPLE 2 ..... 3

SUMMARY ..... 7

ACKNOWLEDGMENT ..... 7

REFERENCES ..... 7

# NEARFIELD DETECTION OF A CROSSING TARGET IN CLUTTER

## INTRODUCTION

Often, in adaptive array analysis, a target is assumed to be moving in the farfield. Matched filter detection of this target in noise is accomplished by accounting for a linear phase shift across the antenna elements owing to their spatial alignment as well as accounting for a linear phase shift from pulse to pulse owing to the Doppler frequency shift of the target. In the nearfield, where the incoming radiation cannot be assumed to be planar, detection of a moving target is more complicated as the phase shifts are generally nonlinear functions of the geometry. A relatively unexplored concept, called spatial Doppler by Skolnik [1], is important in this detection problem. A spatial Doppler phase shift is a phase shift of the received signal at one element relative to the received signal at another resulting from the spatial distribution of the two elements and the target. This phase shift is analogous to the ordinary temporal Doppler phase shift, which is a phase shift at a single element from pulse to pulse. By using two simple examples, this property is demonstrated in the detection of a target in the nearfield that is traveling in the cross-range direction in the presence of narrowband Gaussian clutter.

## EXAMPLE 1

This example considers the detection of a crossing target in the nearfield in Gaussian clutter. A three-element, linear-array antenna with interelement spacing $d$ is used for echo reception. The center element radiates two omnidirectional pulses $T$ seconds apart. The target moves along a line parallel to the array as depicted in Fig. 1. The two pulses strike the target at equidistant points on either side of a perpendicular to the array through the center element. The data vector $\mathbf{x}$ is a six-by-one vector having one entry for each element and each pulse. The zero-mean Gaussian noise is a result of distributed clutter that is uncorrelated from element to element but is correlated from pulse to pulse with correlation coefficient $\rho$. For this example, the covariance matrix $R$ is real and is given by

$$R = \sigma_c^2 \begin{bmatrix} 1 & \rho & 0 & 0 & 0 & 0 \\ \rho & 1 & 0 & 0 & 0 & 0 \\ 0 & 0 & 1 & \rho & 0 & 0 \\ 0 & 0 & \rho & 1 & 0 & 0 \\ 0 & 0 & 0 & 0 & 1 & \rho \\ 0 & 0 & 0 & 0 & \rho & 1 \end{bmatrix}$$

where $\sigma_c^2$ is the variance of the clutter.

By using complex notation for narrowband signals, the Neyman-Pearson optimal detector for signals in Gaussian noise is the matched filter with test statistic

Manuscript approved August 31, 1987.

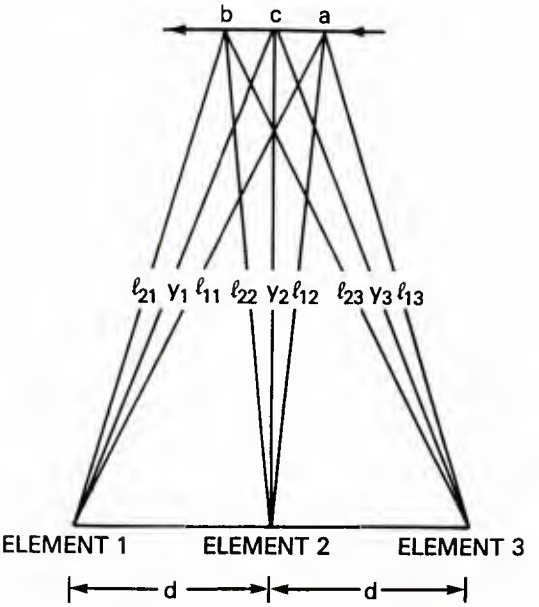


Fig. 1 — Geometry of the moving target and the antenna. Target is at **a** at reflection of first pulse and at **b** at the second. The clutter is distributed in Example 1 and at **c** in Example 2. In both examples, pulse interval $T = 10$ ms, element spacing $d = 30$ ft, and wavelength $\lambda = 1$ ft

$$\lambda_{NP} = \mathrm{Re}\left[\,\bar{\mathbf{s}}' R^{-1}\,\mathbf{x}\right], \tag{1}$$

where **s** is the signal vector, the bar denotes complex conjugation, the prime denotes the transpose, and $R^{-1}$ is the inverse covariance matrix.

Although this example considers only one specific target geometry and motion, the general case is handled by considering a set of target conditions. As in an ordinary "Doppler filter bank," a set of signal vectors is derived that corresponds to the set of target conditions of interest. Next, a bank of parallel matched filters for this set of signal vectors is implemented, and one filter is closely matched to the true target configuration.

The signal vector, which is often called the steering vector, is determined by the differences in distance that the pulses travel to the different elements. The differences are measured relative to a common arbitrary reference length. In this example, the path differences of $\delta_{mn}$ for the $m$th pulse and $n$th element are measured relative to the distance the first pulse travels to reach the center element, which, by symmetry, is the same for the second pulse. The path differences $\delta_{mn}$ are given by

$$\delta_{mn} = \ell_{mn} - \ell_{12} \quad m = 1, 2 \quad n = 1, 2, 3\ ,$$

where $\ell_{mn}$ is the distance of the target at the $m$th pulse to the $n$th element, and the range to the target is defined to be $\ell_{12} = \ell_{22}$. The relative phase shifts $\theta_{mn}$ are related to these path differences and the wavelength $\lambda$ of the pulse by

$$\theta_{mn} = 2\pi\delta_{mn}/\lambda.$$

The signal vector and its components are given by

$$\mathbf{s}' = \left[ s_{11}\ s_{21}\ |\ s_{12}\ s_{22}\ |\ s_{13}\ s_{23} \right],$$

$$s_{mn} = e^{j\theta_{mn}}.$$

Thus, in this example, the center element has zero relative phase shift for the first and second pulse and $s_{12} = s_{22} = 1$.

For this example, the test statistic is

$$\lambda_{\mathrm{NP}} = \mathrm{Re} \left\{ \sum_{n=1}^{3} \left[ \bar{s}_{1n}\ \bar{s}_{2n} \right] \begin{bmatrix} 1 & -\rho \\ -\rho & 1 \end{bmatrix} \begin{bmatrix} x_{1n} \\ x_{2n} \end{bmatrix} \right\} / \sigma_c^2 (1 - \rho^2).$$

For an input signal strength of $b$, the output signal-to-noise ratio ($(S/N)_o$) is given by

$$(S/N)_o = \frac{b^2}{\sigma_c^2 (1 - \rho^2)} \sum_{n=1}^{3} \left[ \bar{s}_{1n}\ \bar{s}_{2n} \right] \begin{bmatrix} 1 & -\rho \\ -\rho & 1 \end{bmatrix} \begin{bmatrix} s_{1n} \\ s_{2n} \end{bmatrix}.$$

For zero velocity, the output signal-to-noise ratio is

$$(S/N)_o \,|_{\mathrm{vel}\,=\,0} = \frac{6b^2}{\sigma_c^2 (1 + \rho)}.$$

Normalizing the output signal-to-noise ratio to the value for zero velocity yields the relative improvement $\gamma$ of detecting a crossing target in clutter. Because of the symmetries in the covariance matrix and in the geometry, the improvement reduces to

$$\gamma = \left[ 3 - \rho - 2\rho \cos (\theta_{21} - \theta_{11}) \right] / 3(1 - \rho).$$

Note that these phase shifts are due to a combination of spatial and temporal Doppler. The overall phase shift cannot be decomposed into a sum of the spatial and temporal Doppler components as the two parts are nonlinearly related through the geometry. This is in contrast with the farfield analysis.

In Fig. 2, the improvement is plotted versus velocity for several different ranges and a correlation coefficient $\rho = 0.999$. The improvement ranges from $\gamma = 0$ dB at certain blind speeds to as much as 31 dB. The improvement increases as the correlation increases as shown in Fig. 3. Both figures illustrate that the above processing yields a significant improvement in the signal-to-noise ratio for a crossing target for which conventional moving target indicator (MTI) processing is ineffective.

## EXAMPLE 2

As in the previous example, the target is moving parallel to a three-element antenna array in the nearfield. However, the noise in this example comes from a single, dominant clutter point. The point source is in the same range cell as the target and is located on the perpendicular to the array through the center element as shown in Fig. 1. The noise is zero-mean Gaussian distributed noise with pulse-to-pulse correlation coefficient $\rho$. The noise is also correlated from element to element

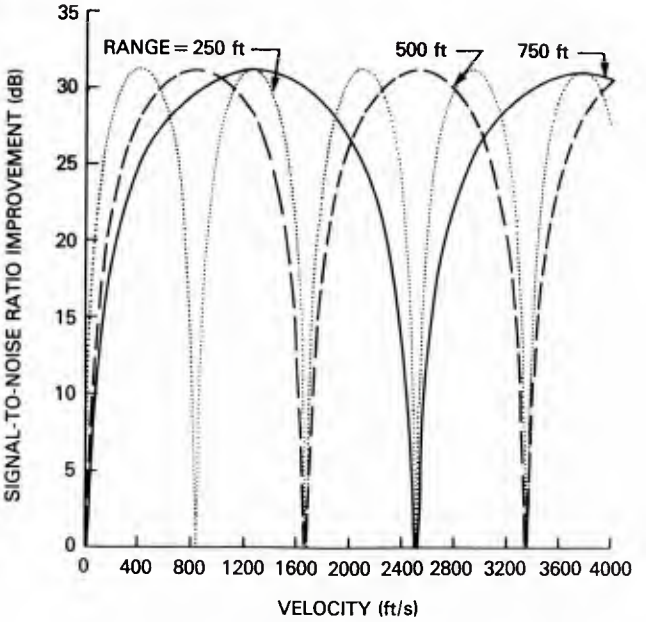


Fig. 2 — Signal-to-noise ratio improvement vs velocity in Example 1 for several target ranges and correlation coefficient $\rho = 0.999$

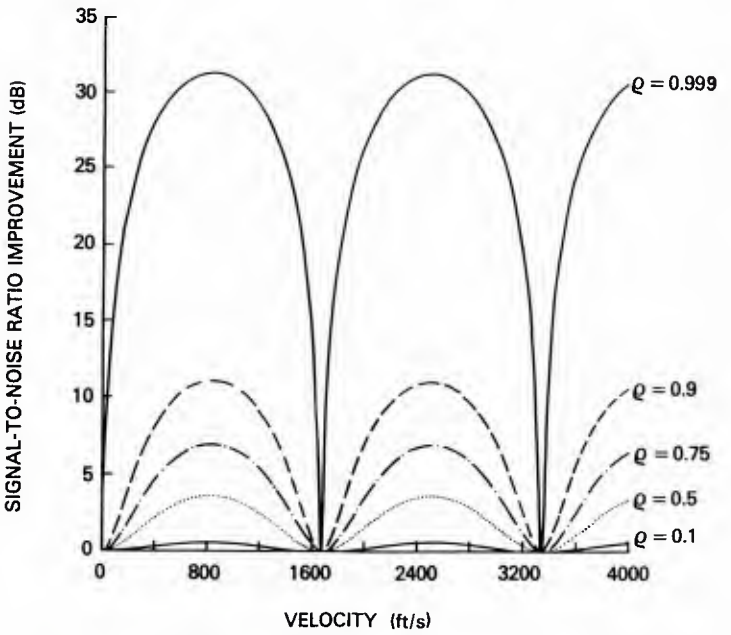


Fig. 3 — Signal-to-noise ratio improvement vs velocity in Example 1 for several correlation coefficients $\rho$ and target range = 500 ft

because of the geometry. Letting $y_n$ be the distance from the clutter point to the $n$th element, the phase shifts $\phi_n$ relative to the noise received at the center element are given by

$$\phi_n = 2\pi(y_n - y_2)/\lambda \quad n = 1, 2, 3,$$

where $\lambda$ is the wavelength of the narrowband noise. If $N_1$ and $N_2$ are the complex random variables for the noise for the two samples in time with common variance $\sigma_c^2$, then the covariance matrix $R_c$ is given by

$$R_c = E\left\{ \begin{bmatrix} N_1 e^{j\phi_1} \\ N_1 \\ N_1 e^{j\phi_3} \\ \text{---------} \\ N_2 e^{j\phi_1} \\ N_2 \\ N_2 e^{j\phi_3} \end{bmatrix} \left[ \bar{N}_1 e^{-j\phi_1} \; \bar{N}_1 \; \bar{N}_1 e^{-j\phi_3} \mid \bar{N}_2 e^{-j\phi_1} \; \bar{N}_2 \; \bar{N}_2 e^{-j\phi_3} \right] \right\} = \sigma_c^2 \begin{bmatrix} R_1 & \rho R_1 \\ \rho R_1 & R_1 \end{bmatrix},$$

where

$$R_1 = \begin{bmatrix} 1 & e^{j\phi_1} & e^{j(\phi_1 - \phi_3)} \\ e^{-j\phi_1} & 1 & e^{-j\phi_3} \\ e^{j(\phi_3 - \phi_1)} & e^{j\phi_3} & 1 \end{bmatrix},$$

$$\sigma_c^2 = E[N_1\bar{N}_1] = E[N_2\bar{N}_2], \text{ and}$$

$$\rho = E[N_1\bar{N}_2]/\sigma_c^2 = E[N_2\bar{N}_1]/\sigma_c^2.$$

Note that the vectors and the matrix are ordered with the components for the three elements at the first pulse coming before the components for the second pulse. This is different than in Example 1. Since this matrix is singular, zero-mean white Gaussian noise is added with variance $\sigma_t^2$ so that the overall covariance matrix $R$ is nonsingular and is given by

$$R = R_c + R_t = R_c + \sigma_t^2 I,$$

where $I$ is the identity matrix. The clutter-to-thermal noise power ratio $\beta$ is defined to be

$$\beta = \sigma_c^2/\sigma_t^2.$$

The Neyman-Pearson optimal detector is again the matched filter as in Ref. 1. The output signal-to-noise ratio for a signal strength $b$ is given by

$$(S/N)_o = b^2 \, \bar{\mathbf{s}}' \, R^{-1}\mathbf{s},$$

where the steering vector s has the same components as in Example 1 but is reordered to reflect the element-to-element then pulse-to-pulse order of the covariance matrix. The improvement in signal-to-noise ratio for a moving target over a stationary one was calculated on a computer and is plotted in Fig. 4 for several values of $\rho$ and a clutter-to-thermal noise power ratio of 20 dB. As shown, the improvement is practically independent of the pulse-to-pulse noise correlation. In Fig. 5, the improvement is plotted for $\rho = 0.9$ and several different clutter-to-thermal noise power ratios.

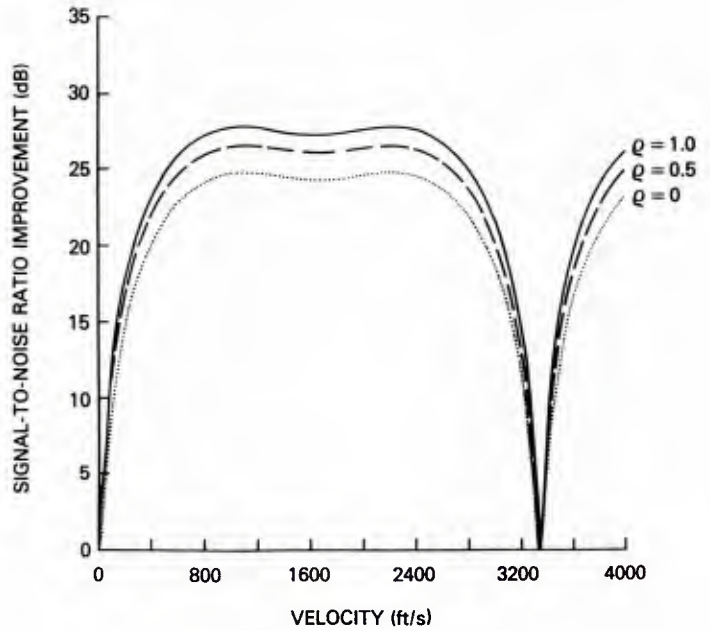


Fig. 4 — Signal-to-noise ratio improvement vs velocity in Example 2 for several correlation coefficients $\rho$, target range = 500 ft, and clutter-to-thermal noise power ratio $\beta$ = 20 dB

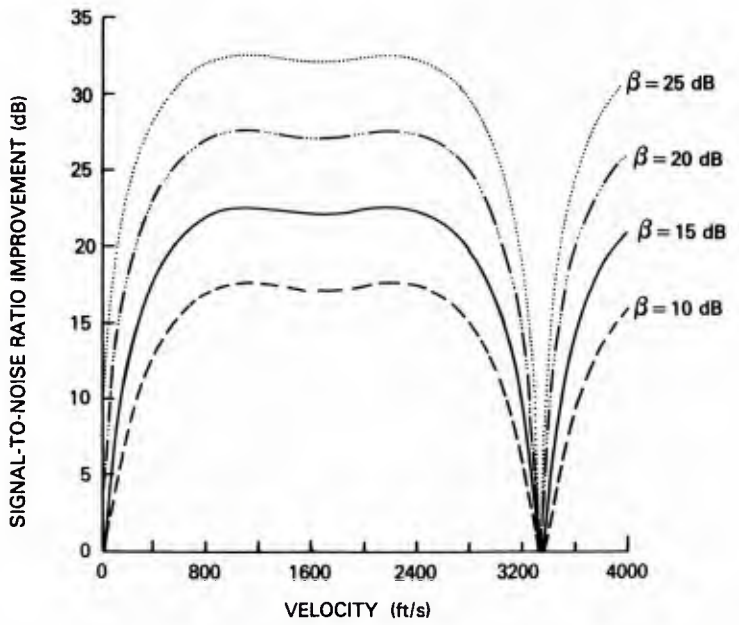


Fig. 5 — Signal-to-noise ratio improvement vs velocity in Example 2 for several clutter-to-thermal noise power ratios $\beta$, target range = 500 ft, and correlation coefficient $\rho$ = 0.9

The results show that the matched filter is placing a null in the beam pattern in the direction of the clutter point. This nearfield problem is similar to the one discussed by Applebaum [2] with a target and a jammer both in the farfield. However, in this example, spatial Doppler is involved in a nonlinear fashion for both the target and the clutter point because they are in the nearfield. Furthermore, this example has pulse-to-pulse motion of the target but with minimal effect as shown by the insensitivity to the clutter correlation. The principal effect of the motion is to provide a spatial separation between the target and the clutter point.

## SUMMARY

Spatial Doppler and temporal Doppler are necessary for the analysis of a target in the nearfield, and the two effects are nonlinearly related through the geometry. By solving the geometry for the detection problem, one can easily find the optimal detector for a signal in Gaussian noise—the matched filter with the steering vector and associated phase shifts. The first example above demonstrated this procedure and showed that the optimal detector yields an improvement in the signal-to-noise ratio for the detection of a crossing target over a stationary one in distributed clutter. The second example made use of the spatial Doppler of the noise as well. Future studies can be conducted with more complicated geometries and different noise environments.

## ACKNOWLEDGMENT

The author thanks Ben Cantrell of the Radar Analysis Branch at the Naval Research Laboratory for his guidance in this investigation.

## REFERENCES

1. M.I. Skolnik, "Radar Information from the Partial Derivatives of the Echo Signal Phase from a Point Scatterer," Naval Research Laboratory Report, to be published.

2. S.P. Applebaum, "Adaptive Arrays," IEEE Trans. Antennas Propag. **AP-24**(5), 585-598, (1976).

DEPARTMENT OF THE NAVY

NAVAL RESEARCH LABORATORY
Washington, D.C. 20375-5000